

## Structure of Micelles Calcium Didodecyl Sulfate: A SAXS Study

Priyadarshi Mahapatra<sup>1\*</sup>, AS Abdul Rasheed<sup>2</sup>, PS Goyal<sup>3</sup> and Jayesh R Bellare<sup>2</sup>

<sup>1</sup>National Energy Technology Laboratory, U.S. Department of Energy, Morgantown, USA

<sup>2</sup>Department of Chemical Engineering, Indian Institute of Technology, Bombay, Powai, Mumbai, India

<sup>3</sup>Pillai's Institute for Information Technology, New Panvel, Mumbai 410206, India

### Abstract

This paper reports the structure of micelles of Calcium Didodecyl Sulfate (CDS),  $\text{Ca}(\text{DS})_2$ , as studied using Small Angle X-ray Scattering (SAXS). CDS is a dianionic surfactant consisting of two DS<sup>-</sup> tails attached to  $\text{Ca}^{++}$  divalent ion. There is considerable interest in understanding the structure (especially the outer shell of counter-ions) of micelles of CDS as unlike conventional surfactants (e.g. CTAB, SDS) where counter-ion is monovalent, CDS has a divalent counter-ion. SAXS is an ideal technique for obtaining information about the outer shell of the  $\text{Ca}(\text{DS})_2$  micelle, as the constituents (S, Ca, O etc.) of the shell are strong X-ray scatterers. The SAXS measurements have been made on salt-free aqueous solutions of calcium didodecyl sulfate for surfactant concentrations of 0.5, 1.0, 2.5, and 20 weight % (or 8.8, 17.7, 44.92 and 438.01 mM/dm<sup>3</sup>) respectively. Single step indirect Fourier transformation method has been utilized to generate particle distance distribution function. It is found that micelles are prolate ellipsoidal in shape. The size parameters of the ellipsoidal micelles have been determined. Other relevant parameters like mean aggregation number and effective fractional charge has been determined by fitting an ellipsoidal shaped core-shell model to the Fourier transformed scattering data. It is seen that increase in surfactant concentration results in lowering of aggregation number, increase of shell thickness and lowering of total charge and probably lowering of water association.

**Keywords:** Small-angle X-Ray scattering; Calcium didodecyl sulfate; Micelles; Ellipsoidal shape model; Core-shell structure; Aggregation numbers

### Introduction

Surfactant molecules (e.g., CTAB, SDS etc.) in dilute aqueous solutions self assemble to form variety of supra-molecular structures such as micelles, vesicles and liquid crystalline structures [1-3]. The simplest aggregate of the surfactant molecules is referred to as a micelle. In general, micelles could be of various shapes and sizes such as spherical, ellipsoidal, cylindrical, thread-like or dislike depending on the architecture of the surfactant molecule [4-6]. For example, while the micelles of conventional surfactants in dilute solutions are spherical, gemini surfactants possess a thread-like shape [4,6]. In fact, this shape is directly dependent on the spacer length [6]. This study deals with aggregation behavior of calcium didodecyl sulfate,  $\text{Ca}(\text{DS})_2$ , which constitutes of a cylindrical monomer [7,8].

Anionic surfactant molecules such as Sodium Dodecyl Sulfate, NaDS, ionize in aqueous solution and the corresponding micelles are aggregates of DS<sup>-</sup> ions [2,9]. The Na<sup>+</sup> ions of NaDS molecules, known as counter-ions, tend to stay near the negatively charged DS<sup>-</sup> micellar surface. Joshi et al. [9] have studied the micellar structures of a series of univalent anionic surfactants (LiDS, NaDS, KDS, RbDS and CsDS) and shown that the size and shape of the micelle is quite sensitive to the change in counter-ion. The study of aggregation behavior of dianionic surfactant  $\text{Ca}(\text{DS})_2$  is of special interest as this particular surfactant provides a system where counter-ions are divalent.

The molecule of dianionic surfactant is cylindrical (Figure 1a) as it consists of two tails attached to a divalent ion [7,8,10,11]. It is crucial to note that monomer of cationic surfactant (Figure 1b), is also cylindrical [12-16] though there are subtle differences between dianionic and cationic surfactants. The dianionic surfactants are formed by mixing of divalent salt in an anionic surfactant solution and removing of unreacted ions [7]. On the other hand, the cationic monomers are formed by mixing of cationic and anionic surfactants [15] and thus there is strong electrostatic interaction between the two head groups. This implies that the nature of bonds and their strengths

in dianionic systems would be different from those found in cationic systems. While the formation of vesicles and flexible cylinders has been seen for cationic surfactants [11,12,16], it is of interest to study the aggregation behavior of dianionic surfactant  $\text{Ca}(\text{DS})_2$ .

Small Angle X-ray Scattering (SAXS) is a well established technique for studying the structure of materials on a length scale of 10-1000 Å simultaneously and this is routinely used for studying structures of micellar solutions [17-19]. It may be mentioned that X-rays scattering power of different elements is different and it almost scales as the atomic number of the element. Thus heavier elements are seen more prominently in presence of light elements. It is this property of X-ray scattering that makes SAXS as an ideal technique for studying core-shell structure of micelles [20,21]. This paper reports the sizes and shapes of  $\text{Ca}(\text{DS})_2$  micelles as obtained from Small Angle X-ray Scattering (SAXS) studies. The following section presents the experimental setup and other relevant details. Details of the proposed model and data analysis involved are given in Section 3. Section 4 shows the results and various insights obtained from this study.

### Experimental Section

#### Materials

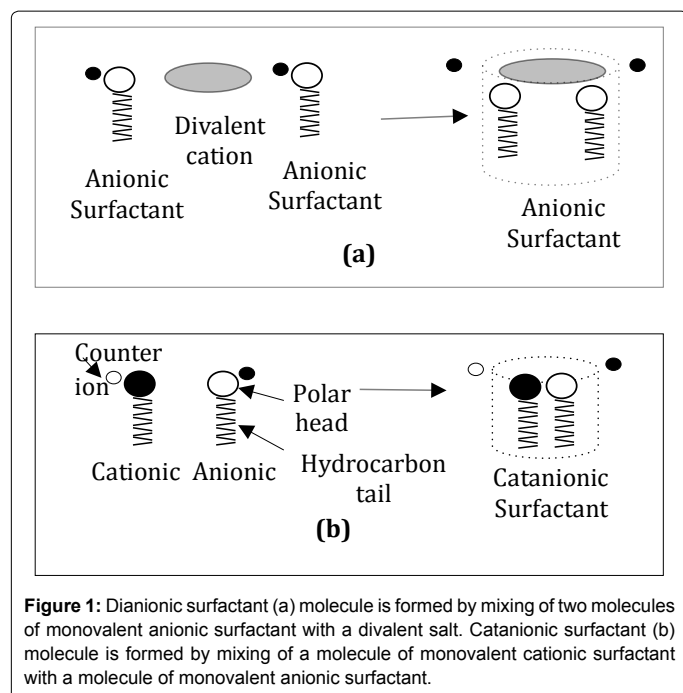
Sodium dodecyl sulfate, SDS ( $M_w=288.38$ , 99% pure, AR grade) purchased from Fluka, Bombay and calcium chloride ( $\text{CaCl}_2 \cdot 2\text{H}_2\text{O}$ ,  $M_w=147.02$ , purity>99%) from Loba Chemie, Bombay were used as

**\*Corresponding authors:** Priyadarshi Mahapatra, National Energy Technology Laboratory, U.S. Department of Energy, Morgantown, WV 26505, USA, Tel: +1.518.618.7351; Fax: +1-304-285-4469; E-mail: [priyadarshi.mahapatra@netl.doe.gov](mailto:priyadarshi.mahapatra@netl.doe.gov)

Received June 23, 2015; Accepted July 20, 2015; Published July 30, 2015

**Citation:** Mahapatra P, Abdul Rasheed AS, Goyal PS, Bellare JR (2015) Structure of Micelles Calcium Didodecyl Sulfate: A SAXS Study. J Nanomed Nanotechnol 6: 307. doi:10.4172/2157-7439.1000307

**Copyright:** © 2015 Mahapatra P, et al. This is an open-access article distributed under the terms of the Creative Commons Attribution License, which permits unrestricted use, distribution, and reproduction in any medium, provided the original author and source are credited.



the raw-materials without further purification. Calcium didodecyl sulfate, CDS, was prepared by mixing SDS and calcium chloride using subsequent centrifugation-redispersion-filtration technique. All the samples were prepared using Millipore ultra pure water (resistivity 18.2 M $\Omega$ .cm). The CDS was obtained as a white precipitate, the mixture was heated to 60°C to complete the reaction and to redissolve the precipitate, then kept for a couple of days to precipitate again and to phase separate out. The conductivity of clear solution was noted (~9.72 mS/cm) and discarded to eliminate the unreacted and other materials. The bottom precipitate layer was redispersed in pure water, heated to 60°C, cooled back to room temperature and centrifuged at 9000 rpm for 20 min at room temperature. The supernatant clear solution was discarded. The procedure was repeated until the conductivity of supernatant solution became less than 1% of the initial clear solution's conductivity. The conductivity of the supernatant solution was found to be 94.7  $\mu$ S/cm (corresponding to 0.00415 mM of NaCl). The precipitate of purified CDS was dried in an oven at 50°C for one week. It was seen that purity of CDS was higher than 98% as determined by atomic absorption inductively coupled plasma (AAS-ICP method).

### SAXS experiments

SAXS experiment involves scattering of a monochromatic beam of X-rays from the sample and measuring the scattered X-ray intensity in a region of small scattering angles. This experiment provides scattered X-ray intensity  $I(q)$  as a function of wave vector transfer  $q (= 4\pi \sin \theta / \lambda)$ , where  $\lambda$  is wave length of incident X-rays and  $2\theta$  is the scattering angle. The typical  $q$  range covered in SAXS studies cover is about 0.001  $\text{\AA}^{-1}$  to 0.5  $\text{\AA}^{-1}$ . The commercial SAXS machines operate with line collimation and those on synchrotron sources use pin-hole geometry. The present studies on micellar solutions of CDS were carried out using SAXSess camera (Anton Paar, Austria) with line collimation. The incident radiation (wavelength=1.542  $\text{\AA}$ ) was Cu K $\alpha$  X-rays from a PANalytical X-ray source (PW3830 X-ray generator) at 40 kV and 40 mA. The scattered X-ray intensities were collected in a two-dimensional position sensitive imaging plate, and integrated over a linear profile to convert into one-dimensional ( $I(q)$  vs.  $q$ ) scattering data. The sample to detector

distance was 264.5 mm. The sample holder used was a capillary made of quartz having inner diameter ~1.5 mm and 10  $\mu$ m thickness. Exposure time was 6 hours per sample. The measurements have been made on micellar solutions of CDS for surfactant concentrations of 0.5, 1.0, 2.5, and 20 weight % (or 8.8, 17.7, 44.92 and 438.01 mM/dm $^3$ ) respectively. All the samples were heated up to 65°C (turbidity disappears) and were maintained at that temperature for 5 min. Thereafter, they were gradually cooled down to room temperature, and reheated to 55°C for SAXS studies. The sample temperature was maintained at  $55 \pm 0.2^\circ\text{C}$  using temperature controller (TCS120, Anton Paar) for all the studies. Scattering data for the background, obtained under similar conditions, was subtracted from the sample data to obtain scattering from self-assembled aggregates of CDS. Millipore ultra pure water was used as reference/background matrix.

### Data Analysis and Model

The intensity  $A(q)$  of X-rays scattered from a micellar solution is expressed in terms of the elementary scattering amplitude  $A(q)$  of the micelles and of the structure factor  $S(q)$  as given in various sources [19,22] as

$$I(q) = n_{mic} \left[ \langle A^2(q) \rangle + \langle A(q) \rangle^2 (S(q) - 1) \right] \quad (1)$$

where,  $n_{mic} = (c - c_M) N_A / n_{ag}$ ,  $n_{mic}$  is the number of micelles per unit volume,  $c$  surfactant concentration,  $c_M$  critical concentration of micelle formation, and  $N_A$  Avogadro's number. The notation  $\langle \rangle$  denotes thermodynamic averaging.  $n_{ag}$ , aggregation number, the number of dodecyl sulfate molecule in a micelle. Scattering amplitude  $A(q)$  depends on size and shape of micelle and the inter-micellar structure factor  $S(q)$  depends on the way micelles are distributed in the solution. In case of dilute solutions, inter-micellar interactions are negligible and the expression for intensity reduces to

$$I(q) = \chi \langle A^2(q) \rangle + B \quad (2)$$

Here  $\chi$ , scaling factor had been introduced to normalize the fitted curves to the maximum intensity values in the experimental scattering data. A constant term ( $B$ ), independent of  $q$ , was introduced to account for any residual incoherent scattering due to background after subtraction. Both  $\chi$  and  $B$  were taken as free-parameters in the data analysis. Depending on the shape or model for the micelle, the expression for scattering amplitude  $A(q)$  can be derived [17,23] depending on the shape and size of the scattering particle.  $A(q)$  depends on the contrast factor, which is decided by the difference in electron density of the particle and that of the solvent. At times, as in case of micelles, different parts of the particle may have different electron densities and this is reflected in expression for  $A(q)$  [24]. For example, when a micelle has core-shell structure, the contrast factor for the shell could be different from that for the core.

### Micellar model and expression for x-ray scattering amplitude

The micelle is modeled as built of two cofocal ellipsoidal shells in line with Borbely et al. [25] with distance  $d$  between their respective semi-major and semi-minor axes [25-27]. That is,  $b_c$  the semi-minor axis of the core and  $b$  is the thickness of the outer shell (Figure 2). The scattering contrast within the inner shell (core region),  $\Delta\rho_c$  and in the region between the two shells (shell region),  $\Delta\rho_{sh}$  were assumed constant. The core contains the dodecyl chains without any water molecules. It is assumed that the entire hydrocarbon chain lies within the core. The core the consisting of hydrocarbon chains is expected to have lower electron density as compared to background matrix i.e. water. The shell region consists of the head-groups ( $\text{SO}_4^-$ ), counter-

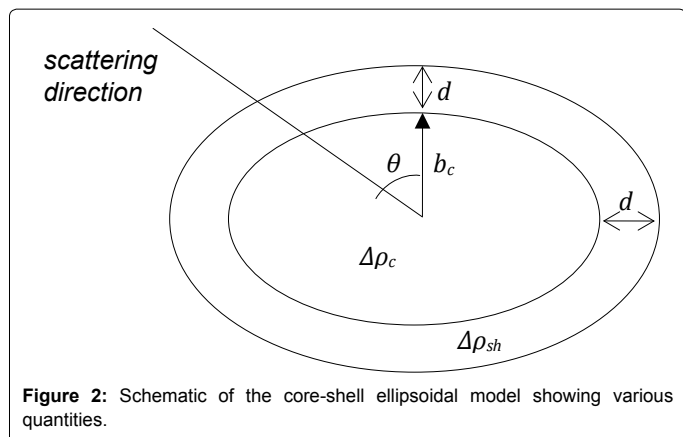


**Figure 2:** Schematic of the core-shell ellipsoidal model showing various quantities.

ions ( $\text{Ca}^{2+}$ ) and solvent-molecules ( $\text{H}_2\text{O}$ ) attached with them. The values for volume of individual molecule/group and hydration numbers for calculating contrast factors  $\Delta\rho_c$  and  $\Delta\rho_{sh}$  have been taken from published literature [18-21]. The hydration number for  $\text{SO}_4^-$  and  $\text{Ca}^{2+}$  were kept constant for all concentrations or molar ratios of the surfactants in the fitting procedure.

The scattering amplitude ( $A$ ) for a two-shell ellipsoid is given as a function of semi-minor axis of the core ( $b_c$ ), axial ratio of the core ( $\zeta$ ), shell thickness ( $d$ ) and  $\theta$ , the angle between scattering vector  $q$  and  $b_c$ .

$$A(q, b_c, \zeta, d, \theta) = \left[ V_C(b_c, \zeta)(\Delta\rho_c - \Delta\rho_{sh})F_C(q, b_c, \zeta, \theta) + V_M(b_c, \zeta, d)\Delta\rho_{sh}F_M(q, b_c, \zeta, d, \theta) \right] \quad (3)$$

where,  $V_C(b_c, \zeta) = 4\pi b_c^3 \zeta / 3$  and  $V_M(b_c, \zeta, d) = 4\pi(b_c + d)^2(b_c \zeta + d) / 3$  are the volumes of the inner and outer ellipsoids respectively. The form factor for the core ( $F_C$ ) and the micelle ( $F_M$ ) is given by

$$F_C(q, b_c, \zeta, \theta) = 3 \frac{\sin R_c q - R_c q \cos R_c q}{(R_c q)^3} \quad (4)$$

$$F_M(q, b_c, \zeta, d, \theta) = 3 \frac{\sin R_m q - R_m q \cos R_m q}{(R_m q)^3} \quad (5)$$

where,  $R_c = b_c \cdot [1 + (\zeta^2 - 1) \cos^2 \theta]$  and  $R_m = b_c \cdot [1 + (\zeta^2 - 1) \cos^2 \theta] + d$

The thermodynamic average scattering amplitude is given by integral over the equally probable orientations given by Eq. 6, which were evaluated numerically.

$$\langle A^2(q, b_c, \zeta, d, \theta) \rangle = \frac{1}{2} \int_0^\pi A^2(q, b_c, \zeta, d, \theta) \cdot \sin(\theta) d\theta \quad (6)$$

The volume of the non-wetted hydrocarbon core ( $V_C$ ) and the whole micelle ( $V_M$ ) was defined as

$$V_C = n_{ag} [V_{CH_3} + 11 \cdot V_{CH_2}] \quad (7)$$

$$V_M = n_{ag} \cdot [V_{SO_4^-} + w_{so_4} V_{H_2O} + (1 - \alpha)(V_{Ca^{2+}} + w_{Ca^{2+}} V_{H_2O})] + V_C \quad (8)$$

where,  $V_{CH_3}$ ,  $V_{CH_2}$ ,  $V_{SO_4^-}$ ,  $V_{Ca^{2+}}$  and  $V_{H_2O}$  are the volumes of hydrocarbon groups ( $\text{CH}_3$  and  $\text{CH}_2$ ), head-group ( $\text{SO}_4^-$ ), counter-ions ( $\text{Ca}^{2+}$ ) and solvent-molecule ( $\text{H}_2\text{O}$ ) respectively.  $w_{SO_4^-}$  and  $w_{Ca^{2+}}$  are the hydration numbers of head-groups and counter-ions, respectively. The volumes and hydration numbers used were taken from various sources [27-30]. Another important free-parameter  $\xi = \Delta\rho_c / \Delta\rho_{sh}$  was introduced to account for scattering lengths in the

core and shell regions. Since these values were not available, Eq. 3 can be re-written as

$$A(q, b_c, \zeta, d, \theta) = \Delta\rho_{sh} [V_C(b_c, \zeta)(\xi - 1)F_C(q, b_c, \zeta, \theta) + V_M(b_c, \zeta, d)F_M(q, b_c, \zeta, d, \theta)] \quad (9)$$

The  $\Delta\rho_{sh}$  term being a constant gets absorbed in the scaling factor term  $\chi$  in Eq. 2, and while evaluating the intensity it does not affect the overall behavior of the model profile. Therefore, absolute values of scattering lengths are not required for this model.

It is customary to obtain Pair Distance Distribution Function (PDDF),  $p(r)$ , from SAXS data and compare it with that based on micellar model.  $p(r)$  can be calculated from the measured X-ray intensity (obtained using Eq. 2) by inverse Fourier transformation and is given by:

$$p(r) = \frac{1}{2\pi^2} \int_0^\infty I(q) \cdot qr \cdot \sin(qr) dq \quad (10)$$

The free parameters were obtained by fitting the model intensity curve to the indirect Fourier transformed form-factor data for the best fit (least square). After the free parameters were determined, dependent parameters ( $n_{ag}$ ,  $\alpha$ ) were computed by simultaneously solving Eqs. 7 and 8. PDDF was obtained from the fitted intensity profile and was compared with PDDF obtained from Indirect Fourier Transformation analysis. An approximate quality of the fit is indicated by  $R^2$ -value, which represents the deviation of the transformation fitted points from the calculated curve.

The  $R^2$  is defined by

$$R^2 = \sum_{i=1}^N \left( \frac{I_{i, \text{model}} - \bar{I}_{i, \text{app}}}{I_{i, \text{app}} - \bar{I}_{i, \text{app}}} \right)^2 \quad (11)$$

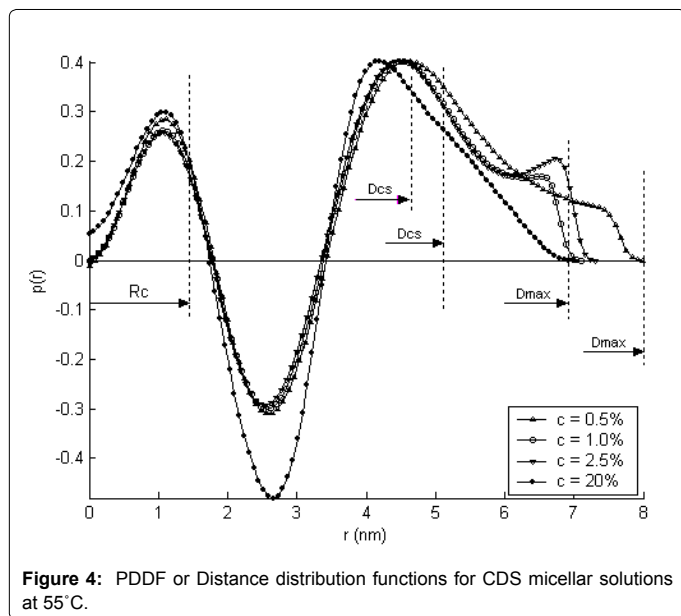
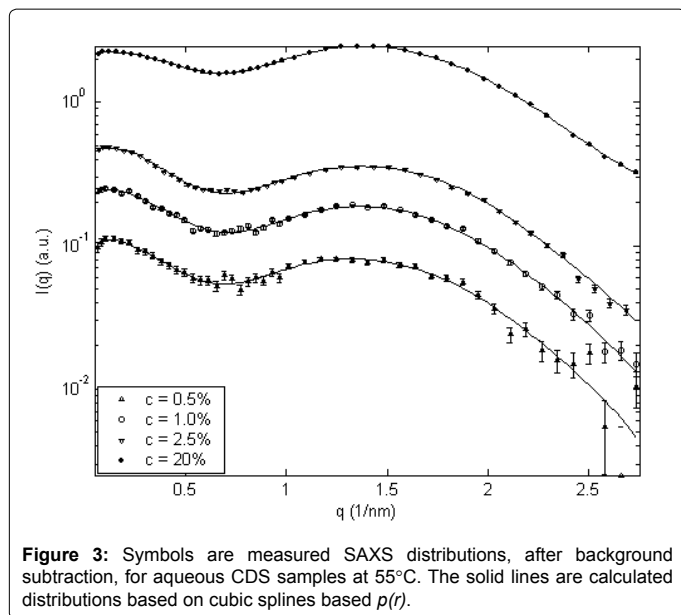
In the above equation  $I_{i, \text{app}}$  and  $I_{i, \text{model}}$  denote the approximated and fitted intensities, respectively,  $\bar{I}_{i, \text{app}}$  is the mean value of the approximated intensities.

## Results and Discussion

### Pair distance distribution function (PDDF)

Figure 3 shows the measured SAXS distributions for all the samples after the data have been corrected for background and empty sample holder contributions. These data along with Eq. 10 were used to calculate the pair distance distribution functions (PDDF) and the results are shown in Figure 4. This involved smoothing and de-smearing the profiles to eliminate deteriorating effects from slit length and slit width. This has been done by computing and fitting the "smoothened" scattering curve to the measured one using the  $p(r)$  function generated by a series of cubic B-splines [31,32]. The solid lines in Figure 3 are based on  $p(r)$ , which was generated using cubic B-splines. And the structure factor which was evaluated assuming hard-sphere model (Percus Yevick approximation with average structure-factor). The PDDF obtained by inverse Fourier Transformation is similar to what one expects from a prolate ellipsoidal micelle with a core shell structure [17].

The above  $p(r)$  is similar to that for elongated particles suggesting that CDS micelles are prolate ellipsoidal. The maximum dimension ( $D_{\text{max}}$ ) of the micelle or the major axis of the ellipsoidal micelle can be obtained from the PDDF as  $p(r)=0$  for  $r \geq D_{\text{max}}$ . Similarly, the radius  $R_c$  of the micellar core and the radius  $R_{cs}$  ( $=R_c + d$ ) or diameter  $D_{cs}$  of shell of counter-ions can be easily identified in the PDDF. It is seen that the value of  $D_{\text{max}}$  or the major axis of micelle decreases with increase



in surfactant concentration. The radius ( $R_c$ ) of micelle core, which signifies the hydrocarbon chain length, decreases with increasing total concentration suggesting that chains are more folded in concentrated solutions. The shell diameter ( $D_{cs}$ ) and the shell thickness also increases with increasing concentration showing higher number of counter-ions attached to the aggregates and hence implying lower effective charge. The presence of a second peak/distortion in the later part of the curves is due to polydispersity of the samples.

#### Fitting of model based theoretical curves to experimental data

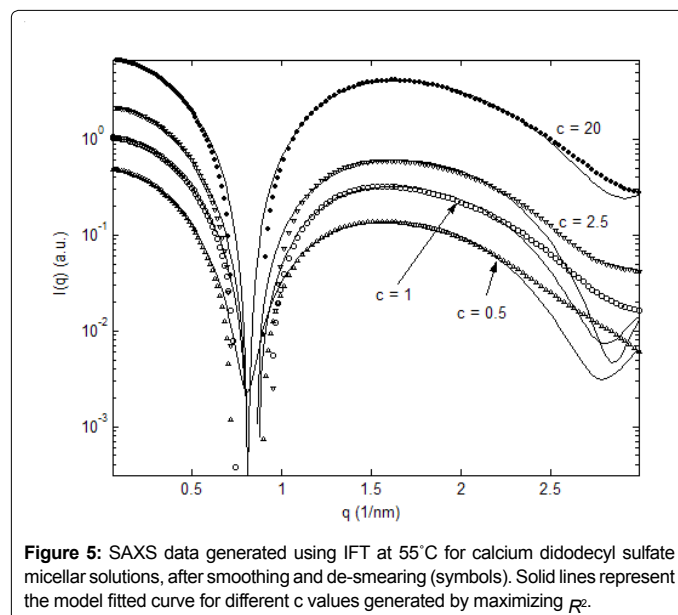
SAXS data have been analyzed in terms of the above mentioned model of the micelle also. That is  $I(q)$  for the above model was calculated and fitted to resolution corrected experimental data with semi-minor

axis of the core ( $b_c$ ), axial ratio of the core ( $\zeta$ ), shell thickness ( $d$ ), background ( $B$ ) and normalizing constant  $\chi$  as parameters. Figure 5 shows the best fitted scattering curves for the ellipsoidal shape models together with the resolution corrected experimental data. The values of the fitted parameters are given in Table 1. It is seen that calculated curves agree very well with the experimental data except at high  $q$  values.

It can be seen that the semi-minor axis of the core, axial ratio and the shell thickness decrease with increasing surfactant concentration. The maximum dimension which denotes the major axis of the whole micelle equaling  $2(b_c\zeta + d)$  obtained are 9.29, 8.69, 8.00 and 7.63 nm, respectively for 0.5, 1, 2.5 and 20 wt% surfactant. These values are about 1 nm larger than those obtained from experimental PDDF. The core radius at all concentrations is similar to those obtained from PDDF although it is smaller than the expected hydrocarbon chain length, showing possible chain folding in these systems [27].

It is interesting to note that axial ratio of ellipsoidal micelle decreases with increasing concentration. From the trend, it is expected that the particle might exist as rod-like structures at very low concentration. The ratio of scattering lengths  $\Delta\rho_c/\Delta\rho_{sh}$  decreases very slightly with increasing surfactant from which it can be inferred that some water molecules are present in the core region and their amount increases with increasing concentration. There is a decrease both in aggregation number and the effective fractional charge associated with each micelle for increasing total surfactant concentration. This decrease in fractional charge is probably responsible for the increase of shell thickness due to presence of attached counter-ions. We also notice that total charge on each micelle decreases by 3 times upon increasing concentration from 0.5 to 20 wt%.

PDDF based on above model has also been compared with the experimentally obtained PDDF and there is reasonable agreement between them. Figure 6 shows the experimental and the calculated PDDF for 0.5% micellar solutions at 55°C. It can be seen that the model can perfectly simulate the initial part (low  $r$ ) of the PDDF curve, which is connected with the inner core dimensions. In later part of the curve, a peak occurs in the fitted curve at lower values of  $r$  but it extends and terminates at higher  $r$  values as compared to experimental



Total surfactant $c$ (wt %)	Semi-minor axis of core $b_c$ (nm)	Axis ratio of core $\zeta$	Shell thickness $d$ (nm)	$\Delta\rho_c/\Delta\rho_{sh} = \xi$	Background $B$	Normalizing factor $\chi$	$n_{ag}$	$\alpha$	$R^2$
0.5	1.459	2.3911	1.1574	-1.5729	-0.0133	1.50E-03	89	0.325	0.9827
1	1.428	2.2324	1.1609	-1.702	-0.0302	4.20E-03	78	0.29	0.9819
2.5	1.3932	2.031	1.172	-1.7096	-0.0745	0.018	66	0.236	0.9802
20	1.3324	1.9774	1.1828	-2.3509	-0.1510	0.059	56	0.171	0.9948

Table 1: Best fitted free parameters for calcium didodecyl sulfate micellar solutions for different concentrations at 55°C.

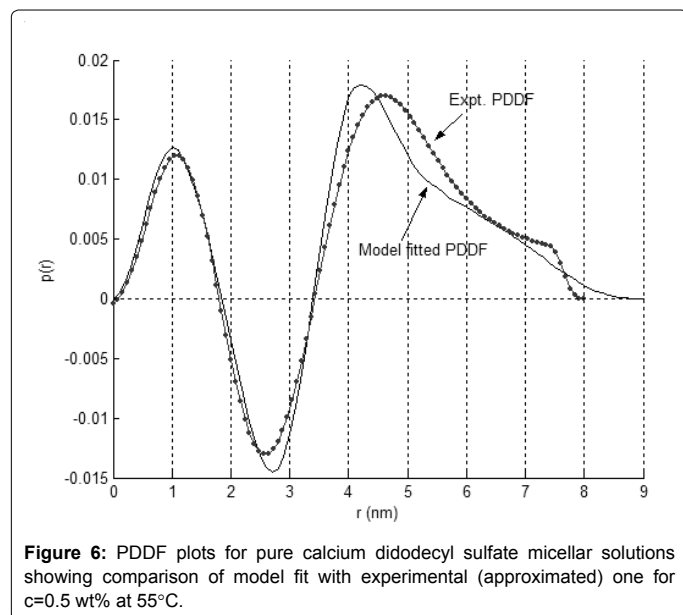


Figure 6: PDDF plots for pure calcium didodecyl sulfate micellar solutions showing comparison of model fit with experimental (approximated) one for  $c=0.5$  wt% at 55°C.

one. This indicates that the value of shell thickness  $d$  obtained from the fit is slightly lower (the inflexion point near the second peak roughly denotes semi-minor axis of the micelle [24]) compared to actual system. The fitted curve also gives higher maximum dimension of the micelle. It may be mentioned that agreement between experimental PPDF and the model based theoretical PPDF was better up to large  $q$  values for concentrated solutions. This shows that experimental PPDF as obtained from Fourier transform of  $I(q)$  data can be fruitfully used for obtaining qualitative information about the aggregate.

## Conclusions

Calcium didodecyl sulfate (CDS) powder has been prepared and its purity was quantified using conductivity measurements and inductive coupled plasma methods. Micellar solutions were prepared by dissolving appropriate quantities of CDS powder in water. The structure of micelles of CDS for several different surfactant concentrations have been studied using SAXS. The qualitative information about the shape and size of micelle was obtained by generating the pair distance distribution function (PDDF) by indirect Fourier transformation method. It was found that CDS micelle is ellipsoidal in shape and its core-shell structure was clearly indicated in PDDF. The values of various size and structural parameters of the micelle have been obtained by fitting the scattering data to a core and shell ellipsoidal micellar model. These studies show that size (aggregation number and major axis of micelle) of micelle in CDS solutions decreases with increase in surfactant concentration. Further it was seen that micellar charge also decreases with increase in surfactant concentration.

## References

- Tanford C (1980) "The Hydrophobic Effect: Formation of Micelles and Biological Membranes," 2nd Ed., Wiley, New York.
- Lindman B, Wennerström H (1980) Miceles. Amphiphile aggregation in aqueous solution. Top Curr Chem 87: 1-87.
- Degiorgio V, Corti M (1985) "Physics of Amphiphiles--micelles, Vesicles, and Microemulsions, Varenna on Lake Como, Villa Monastero," North-Holland, Amsterdam 90.
- Danino D, Talmon Y, Zana R (1995) "Alkanediyl- $\alpha,\omega$ -Bis(Dimethylalkylammonium Bromide) Surfactants (Dimeric Surfactants). 5. Aggregation and Microstructure in Aqueous Solutions," Langmuir 11: 1448-1456.
- Haldar J, Aswal VK, Goyal PS, Bhattacharya S (2001) "Role of Incorporation of Multiple Headgroups in Cationic Surfactants in Determining Micellar Properties. Small-Angle-Neutron-Scattering and Fluorescence Studies". J Phys Chem B 105: 12803-12808.
- Aswal VK, De S, Goyal PS, Bhattacharya S, Heenan RK (1998) "Small-angle neutron scattering study of micellar structures of dimeric surfactants." Phys Rev E E57: 776.
- Zapf A, Hammel R, Platz G (2000) Colloids and Surfaces 213: 184-185.
- Zapf A, Bech R, Platz G, Hoffman H (2003) "Calcium surfactants: A review." Adv Colloid Inter Sci 100-102: 349-380.
- Joshi JV, Aswal VK, Goyal PS (2007) "Combined SANS and SAXS studies on alkali metal dodecyl sulphate micelles." J Phys Condensed Matter 19: 196219.
- Wang J, Song A, Jia X, Hao J, Liu W, et al. (2005) Two routes to vesicle formation: metal-ligand complexation and ionic interactions. J Phys Chem B 109: 11126-11134.
- Song A, Jia X, Teng M, Hao J (2007) Ca<sup>2+</sup>- and Ba<sup>2+</sup>-ligand coordinated unilamellar, multilamellar, and oligovesicular vesicles. Chemistry 13: 496-501.
- Koehler RD, Raghavan SR, Kaler EW (2000) "Microstructure and Dynamics of Wormlike Micellar Solutions Formed by Mixing Cationic and Anionic Surfactants." Journal of Physical Chemistry B 104: 11035-11044.
- Brasher LL, Kaler EW (1996) "A Small-Angle Neutron Scattering (SANS) Contrast Variation Investigation of Aggregate Composition in Catanionic Surfactant Mixtures," Langmuir 12: 6270-6276.
- Zemb T, Dubois M, Deme B, Gulik-Krzywicki T (1999) Self-assembly of flat nanodiscs in salt-free cationic surfactant solutions. Science 283: 816-819.
- Dubois M, Demé B, Gulik-Krzywicki T, Dedieu JC, Vautrin C, et al. (2001) Self-assembly of regular hollow icosahedra in salt-free cationic solutions. Nature 411: 672-675.
- Kaler EW, Murthy AK, Rodriguez BE, Zasadzinski JA (1989) Spontaneous vesicle formation in aqueous mixtures of single-tailed surfactants. Science 245: 1371-1374.
- Glatter O, Kratky O (1982) "Small Angle X-ray Scattering." Academic Press, London 167-196.
- Linder P, Zemb T (1991) "Neutron, X-ray and light scattering: introduction to an investigative tool for colloidal and polymeric systems," North Holland, Amsterdam.
- Lipfert J, Columbus L, Chu VB, Lesley SA, Doniach S (2007) Size and shape of detergent micelles determined by small-angle X-ray scattering. J Phys Chem B 111: 12427-12438.
- Wu CF, Chen SH, Shih LB, Lin JS (1988) Direct measurement of counterion

- distribution around cylindrical micelles by small-angle x-ray scattering. *Phys Rev Lett* 61: 645-648.
21. Aswal VK, Goyal PS, De S, Bhattacharaya S, Amenitsch H, et al. (2000) "Small-angle X-ray scattering from micellar solutions of gemini surfactants." *Chem Phys Lett* 329: 336-340.
  22. Hayter JB, Penfold J (1981) "Self-consistent structural and dynamic study of concentrated micelle solutions." *J Chem Soc Faraday Trans* 77: 1851-1863.
  23. Windsor CG (1988) "An introduction to small-angle neutron scattering." *J Appl Cryst* 21: 582-588.
  24. Jacrot B (1976) "The study of biological structures by neutron scattering from solution." *Rep Prog Phys* 39: 911.
  25. Borbely S, Cser L, Vass Sz, Bezzabotnov, V Yu, Ostanevich et al. (1993) "Micelle formation in sodium hexadecyl sulfate surfactant solutions studied by small-angle neutron scattering." *Colloid Polym Sci* 271: 786-792.
  26. Berr SS (1987) "Solvent isotope effects on alkytrimethylammonium bromide micelles as a function of alkyl chain length." *J Phys Chem* 91: 4760-4765.
  27. Berr SS, Coleman MJ, Jones RRM, Johnson Jr JS (1986) "Small-angle neutron scattering study of the structural effects of substitution of tetramethylammonium for sodium as the counterion in dodecyl sulfate micelles." *J Phys Chem* 90: 6492-6499.
  28. Vass Sz, Torok T, Jakli G, Berecz E (1989) "Sodium alkyl sulfate apparent molar volumes in normal and heavy water: Connection with micellar structure" *J Phys Chem* 93: 6553-6559.
  29. Jalilehvand F, Spångberg D, Lindqvist-Reis P, Hermansson K, Persson I, et al. (2001) Hydration of the calcium ion. An EXAFS, large-angle x-ray scattering, and molecular dynamics simulation study. *J Am Chem Soc* 123: 431-441.
  30. Pavlov M, Siegbahn PEM, Sandstrom M (1998) "Hydration of Beryllium, Magnesium, Calcium, and Zinc Ions Using Density Functional Theory." *J Phys Chem* 102: 219-228.
  31. Glatter O (1977) "A new method for the evaluation of small-angle scattering data." *J Appl Cryst* 10: 415-421.
  32. Glatter O (1979) "The interpretation of real-space information from small-angle scattering experiments." *J Appl Cryst* 12: 166-175.